ACS APPLIED MATERIALS & INTERFACES

RESEARCH ARTICLE

www.acsami.org

Electrospun Polyvinylpyrrolidone Fibers with High Concentrations of Ferromagnetic and Superparamagnetic Nanoparticles

Minoru Miyauchi,[‡,⊥,#,†] Trevor J. Simmons,[§,⊥,#,†] Jianjun Miao,[‡,⊥,#,†] Jennifer E. Gagner,[‡,⊥,#] Zachary H. Shriver,[||] Udayanath Aich,[||] Jonathan S. Dordick,[‡,⊥,#] and Robert J. Linhardt*[,‡,§,⊥,#]

[‡]Chemical and Biological Engineering, [§]Department of Chemistry and Chemical Biology, [⊥]Center for Biotechnology and Interdisciplinary Studies, and [#]Rensselaer Nanotechnology Center, Rensselaer Polytechnic Institute, Troy, New York 12180, United States

[||]Department of Biological Engineering, Harvard-MIT Division of Health Sciences & Technology, Koch Institute for Integrative Cancer Research, Massachusetts Institute of Technology, 77 Massachusetts Avenue, Cambridge, Massachusetts 02139, United States

ABSTRACT:

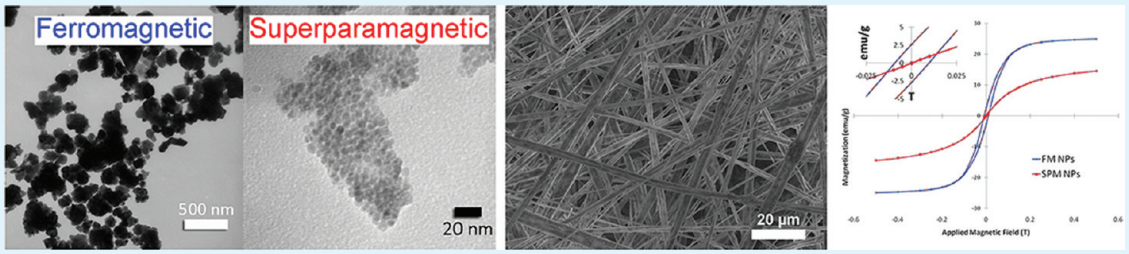

Electrospun polymer fibers were prepared containing mixtures of different proportions of ferromagnetic and superparamagnetic nanoparticles. The magnetic properties of these fibers were then explored using a superconducting quantum interference device. Mixed superparamagnetic/ferromagnetic fibers were examined for mesoscale magnetic exchange coupling, which was not observed as theoretically predicted. This study includes some of the highest magnetic nanoparticle loadings (up to 50 wt %) and the highest magnetization values (≈ 25 emu/g) in an electrospun fiber to date and also demonstrates a novel mixed superparamagnetic/ferromagnetic system.

KEYWORDS: electrospun fibers, superconducting quantum interference device, superparamagnetic fibers, ferromagnetic fibers

INTRODUCTION

Magnetic nanoparticles (NPs) have many important applications including high-density data storage,[1] ultrasensitive sensors,[2] and numerous potential biomedical applications including the treatment of certain cancers.[3] Magnetic NPs can be either ferromagnetic or antiferromagnetic, and very small ferromagnetic (FM) NPs (typically with a diameter <15 nm) can exhibit superparamagnetic (SPM) properties. This breadth of available magnetic nanomaterials offers an exciting opportunity to create mixed magnetic systems having unique properties that may afford advantages over traditional bulk magnetic materials. The incorporation of SPM NPs in a FM or antiferromagnetic matrix can result in magnetic coupling between the materials and represents an approach that has generated increasing interest over the past decade. For example, Skumryev et al.[4] showed that there was significant magnetic exchange coupling between SPM NPs and an antiferromagnetic host matrix, that enabled magnetization stability. Such magnetic coupling would cause the SPM NPs to be influenced by the magnetic moment of the nearest FM NP. This would result in a remnant magnetization in the SPM NPs, referred to as magnetic stabilization.

In the current study, we use electrospun polymer fibers incorporated with NPs, as a model system to investigate the possible interaction of FM NPs with SPM NPs, and the affect on electrospinning conditions. Electrospinning is an excellent method to prepare continuous, quasi-one-dimensional fibers with diameters ranging from nanometers to micrometers by spinning a polymer solution at high speed using electrostatic charging.[4] These fibers have very high surface area to volume ratios, which make them ideal candidates for tissue engineering,[5] conductive nanowires,[6] supercapacitors,[7] nanosensers,[8] and filtration membranes.[9,10] Several types of hybrid nanofibers have been fabricated using electrospinning by incorporating functional nanomaterials or their precursors into polymer solutions.[11] Examples include conductive carbon nanotubes embedded into matrix polymers or in the cores of core−sheath fibers,[12,13] precursors such as titanium-containing compounds dissolved in a polyvinylpyrrolidone solution to yield titania fibers upon calcination,[14] and NPs such as silver and iron oxides introduced into polymer fibers by adding them to the electrospinning solution.[15,16] Fibers containing magnetic NPs have potential uses as smart fibers and fabric for many applications, including magnetic filters,[17] sensors,[18] magnetic shielding devices, and magnetic induction devices.[19]

We are examining the behavior of FM magnetite (Fe_3O_4) NPs of various diameters embedded in electrospun polymer fibers at various loadings. The possible interactions between FM and

Received: February 12, 2011
Accepted: May 11, 2011
Published: May 11, 2011

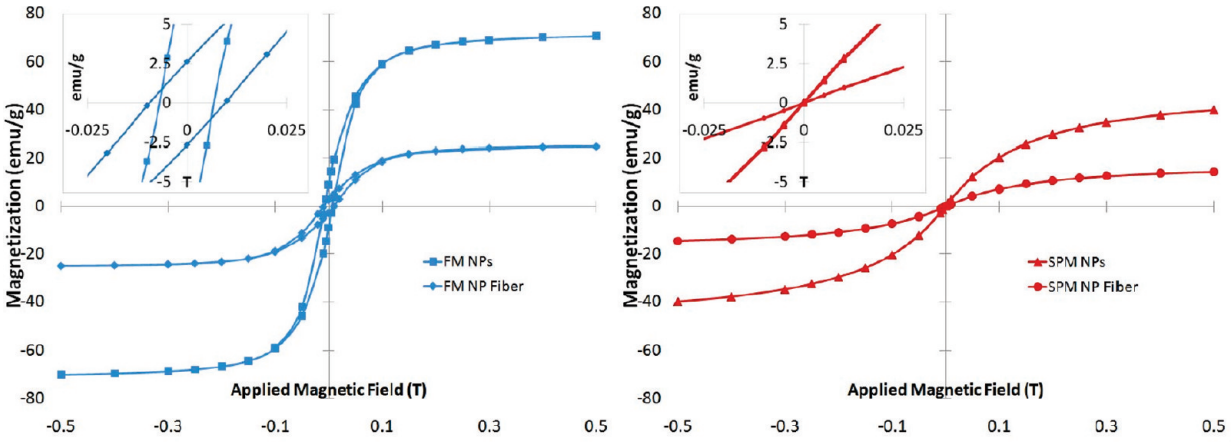

Figure 1. Response of magnetic nanoparticles and electrospun fiber mat samples containing either ferromagnetic nanoparticles (FM NPs) or superparamagnetic nanoparticles (SPM NPs) in a superconducting quantum interferometer device (SQUID). The absence of any significant hysteresis in the magnetization curve for the SPM NPs confirms their superparamagnetic character, and the noticeable hysteresis of the FM NPs is characteristic of small ferromagnetic particles.

SPM Fe_3O_4 NPs by magnetic coupling are of interest as well, as the SPM NPs have the potential to align their magnetic moments with that of the nearest FM NPs. The magnetic properties of the magnetic NP-loaded fibers were then examined using a superconducting quantum interference device (SQUID).

EXPERIMENTAL SECTION

Materials. Polyvinyl pyrrolidone (PVP, MW = 1 300 000) was purchased from Sigma-Aldrich (St. Louis, MO). FM Fe_3O_4 NPs (200 nm in diameter, 96−98% in purity) was purchased from Polysciences, Inc. (Warrington, PA). SPM Fe_3O_4 NPs (5 nm in diameter, including 30 wt % oleic acid) was purchased from NN-Laboratories (Fayetteville, AK). 2-Propanol was from Sigma-Aldrich (St. Louis, MO). All the materials were used as-received without further treatment.

Electrospinning Experiment. Fe_3O_4 NPs in 2-propanol was sonicated for 1 h to obtain good dispersions. Then the required quantity of PVP was added into Fe_3O_4/2-propanol dispersion. The PVP concentration in PVP/2-propanol solution was fixed at 10.7 wt %. PVP/Fe_3O_4/2-propanol solutions were mechanically stirred at room temperature to form homogeneous solutions.

NP-polymer solutions were loaded in a 5 mL syringe equipped with a 0.94 mm (inner diameter) stainless steel gauge needle. The needle was connected to a high voltage supply (CZE1000R, Spellman, Hauppauge, NY), which is capable of generating a DC voltage up to 30 kV. Grounded flat aluminum foil (20 μm thick) was used as collector electrode. The distance between needle and aluminum collector was 18 cm. Solution was constantly fed using a syringe pump (NE-1000, New Era Pump System Inc., Wantagh, NY) at 60 μ/min. Applied voltage was optimized to obtain good spinnability, with typical value of 10−12 kV. Collected fibers on aluminum foil were dried completely under vacuum prior to further investigation.

Characterization. Transmission electron microscopy (TEM) was performed with a Philips CM12 (Eindhoven, Amsterdam, Netherlands) at an accelerating voltage of 120 kV in bright-field mode. Dispersed magnetic NPs on 400 mesh TEM grids were obtained by scooping particles in an ethanol solution with a grid and then drying in vacuum oven for overnight. Electrospun fibers on 400 mesh TEM grids were prepared by electrospinning fibers onto grid for approximately 3 s.

Field emission−scanning electron microscopy (FE-SEM) was performed to study the surface morphology of fibers with a JEOL JSM-6338 FE-SEM (Tachikawa, Tokyo, Japan) equipped with a secondary electron detector at an accelerating voltage of 10 kV and at working distance of 15 mm. Prior to performing the FE-SEM analysis, fibers were coated with gold by sputtering to form a conductive film.

Thermogravimetric analysis (TGA) was performed using a computer controlled TA Instruments TGA Q50 (New Castle, DE). The temperature was ramped up at 10 °C/min up to 700 °C with the furnace open to allow airflow along with nitrogen purge gas.

X-ray diffraction (XRD) spectra were collected using a Bruker AXS D8 Discover diffractometer (Madison, WI) operating with a Cu-Kalpha radiation source (landa =1.54 A). XRD scans were recorded from 20 to 80° for 2θ with 0.02°/step and 0.1 s per step.

The superconducting quantum interference device (SQUID) measurements at 300 K were performed using a MPMS-5S magnetometer (Quantum Design Inc., San Diego, CA) housed at Massachusetts Institute of Technology. Fiber samples were scanned with an applied magnetic field ranging from −0.5 to 0.5 T. Extrapolated saturation magnetization was obtained from the intercept of magnetization versus H^{-1} at high field.

RESULTS AND DISCUSSION

In principle, any FM material will be exhibit paramagnetic behavior above its blocking temperature.[20] This means that with enough thermal motion, any FM material will align its magnetic moments with an external magnetic field. Unlike typical ferromagnetic materials, superparamagnetic materials have very low blocking temperatures. When a FM material, such as magnetite (Fe_3O_4), is sufficiently small (i.e., below a critical diameter), it contains a single magnetic domain with all the magnetic moments of the constituent atoms aligned.[21] Such a FM NP can be viewed as a single giant magnetic moment, known as the macrospin approximation. In superparamagnetism, sufficiently small FM NPs below this critical diameter will not maintain remnant magnetization after being exposed to an external magnetic field, while FM NPs above this critical diameter will maintain a remnant magnetization. This concept is illustrated in Figure 1, which shows magnetic data from a very sensitive magnetometer known as a SQUID. The SQUID magnetometer applies an external magnetic field to a sample in a controlled environment and then measures the resultant magnetization of the sample. The fiber mat sample containing FM NPs shows a small hysteresis loop at low applied magnetic field values, which is

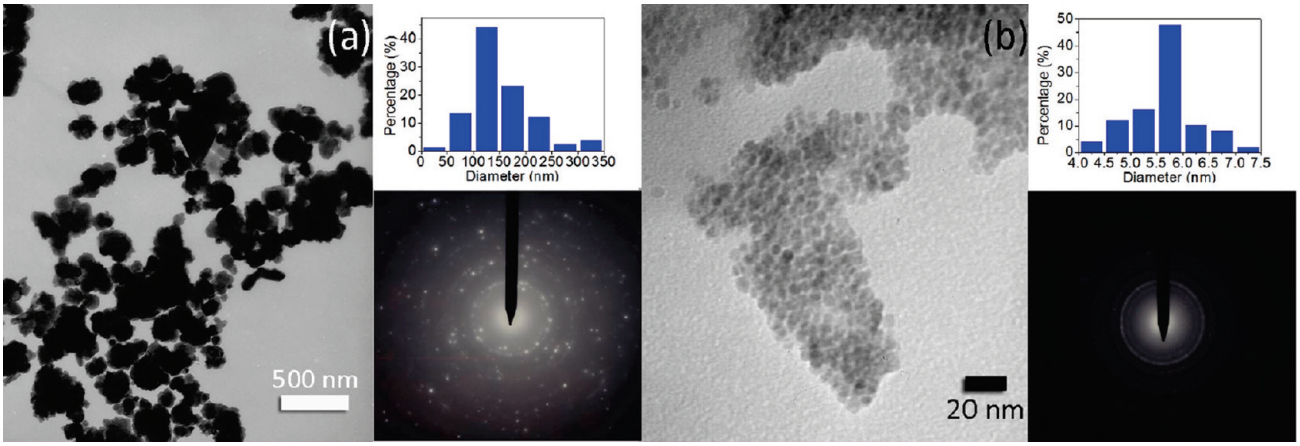

Figure 2. TEM of (a) relatively large FM NPs and (b) much smaller NPs, along with histograms of particle diameter and selected area electron diffraction (SAED) patterns.

characteristic of FM materials. The fiber mat sample containing SPM NPs shows no hysteresis loop, which is characteristic of SPM materials.

The critical diameter of magnetite (Fe_3O_4) has an approximate value of 18.7 nm, assuming a crystalline anisotropy constant of 30 kJ/m^3.[22] NPs with diameters less than 18.7 nm begin to exhibit SPM properties. For this reason, particles with approximate diameters well above and as far below this critical limit were selected in the current studies. These FM Fe_3O_4 NPs and SPM Fe_3O_4 NPs were analyzed by transmission electron microscopy (TEM) (Figure 2).

After an initial empirical evaluation of the diameters, the NP diameters were confirmed by X-ray diffraction. The large FM NPs showed a broad diameter distribution with an average diameter of 151 nm ±59.4 nm (Figure 2a), which is well above the established critical diameter for Fe_3O_4. This broad distribution of diameters is principally due to the production process that involves colloidal milling. SPM NPs synthesized by a thermal decomposition in the presence of oleic acid showed a narrow diameter distribution with average diameter of 5.6 ± 0.6 nm (Figure 2b), which is well below the critical diameter.

Electrospun polymer fibers containing Fe_3O_4 NPs have been previously reported as a means of exploiting the magnetic properties of these NPs.[23−28] In previous investigations, only relatively small diameter NPs, ranging from 4 to 13 nm, were used. These smaller NPs were likely selected because of the ease of fiber fabrication with small NPs when using an electrospinning process. As expected, based on the aforementioned discussion, the resulting fibers exhibited only SPM properties at room temperature. It is considerably more challenging to incorporate relatively large NPs, such as the ∼200 nm in diameter Fe_3O_4 NPs used in the present work, into micrometer or nanometer scale fibers. Despite the difficulties in electrospinning such large NPs, the opportunity to create mixed FM/SPM systems with high NP loadings in a narrow quasi-one-dimensional fiber represents an attractive concept. A majority of the published work does not exceed NP loadings of about 20 wt %, with the reports of higher loadings near 20−30% typically showing significant agglomeration.[29] Wang et al. prepared fibers that reportedly had up to 75 wt % Fe_3O_4 NP loading, and although this is the highest loading found in the literature, no confirmations of such high loadings being possible were presented nor discussed.[30]

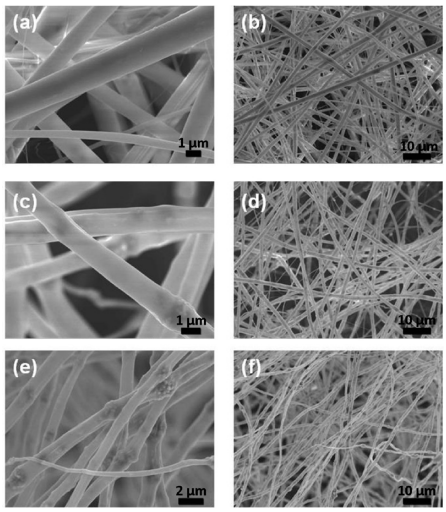

Figure 3. SEM images of PVP fibers loaded with FM NPs: (a, b) PVP/NPs = 95/5 wt %, (c, d) PVP/NPs = 75/25 wt %, (e, f) PVP/NPs = 50/50 wt %.

It is particularly difficult to homogeneously disperse magnetic NPs in a polymer matrix due to the differences in density and polarity of the NPs and polymer. Thus, polyvinylpyrrolidone (PVP) was used as matrix polymer to obtain a more uniform dispersion of NPs. PVP is widely used in the fabrication of fibers through electrospinning, owing to its favorable solubilizing characteristics as a carrier for small particulates. PVP is a good dispersant for many kinds of small molecules and particles, such as functional organic molecules,[31] carbon black,[32] and metal oxide NPs or nanorods,[28,33,34] and can be used to fabricate a variety of composite fibers by electrospinning. Chuangchote et al. prepared PVP fibers using seven different solvents including methanol, ethanol and 2-propanol.[35] Among these solvents, methanol, which had the highest dielectric constant and the lowest viscosity, was the best solvent, providing fibers with a uniform morphological appearance and a small fiber diameter (∼274 nm).

Based on these promising results using methanol as a solvent for PVP electrospinning, we selected methanol as the solvent to obtain thin quasi-one-dimensional fibers containing magnetic NPs. Unfortunately, during electrospinning experiments with high loadings of magnetic NPs (e.g., 50 wt %), a significant

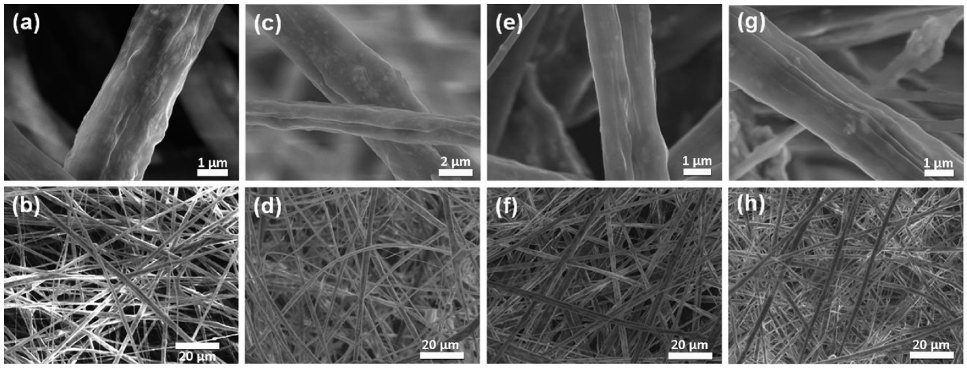

Figure 4. SEM images of PVP fibers containing mixtures of FM and SPM NPs: (a, b) PVP/FM/SPM = 50/0/50 wt %, (c, d) 50/15/35 wt %, (e, f) 50/25/25 wt %, (g,h) 50/35/15 wt %.

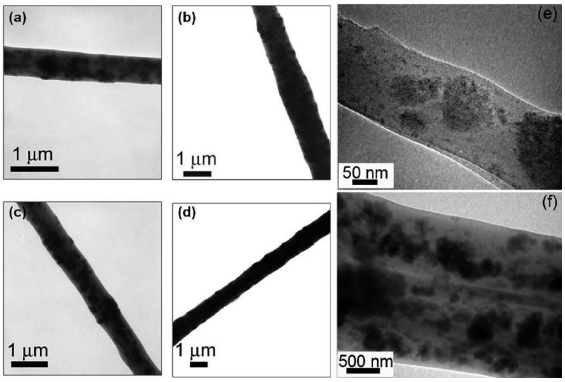

Figure 5. TEM images of PVP fibers containing the mixture of FM and SPM NPs: (a) PVP/FM NPs/SPM NPs. = 50/0/50 wt %, (b) 50/15/35 wt %, (c) 50/25/25 wt %, (d) 50/35/15%. (e, f) High-resolution TEM images showing the presence of SPM NP clusters (e) in a thinner fiber of 50/50 wt %, and FM NPs surrounded by SPM NPs in a thicker fiber of 50/50 wt %.

portion of the NPs appeared to remain in the Taylor cone at the tip of the spinneret during electrospinning. This observation was confirmed with thermogravimetric analysis (TGA), as the NP loadings in the resultant electrospun fibers were lower than that of the initial electrospinning solutions. Because of this complication, 2-propanol was substituted for methanol to obtain higher loadings of NPs while maintaining a stable spinning condition. It is possible that the high solubility of the surfactant on the surface of the SPM NPs (oleic acid) in methanol may have partially contributed to the agglomeration observed, and that changing the solvent to 2-propanol prevented this from occurring. Although the fibers obtained were relatively thicker in comparison to PVP control fibers spun from methanol, FM NPs and mixtures of FM NPs and SPM NPs could be successfully incorporated into PVP electrospun fibers at up to 50 wt % loading.

Characterization of Electrospun PVP-Fe_3O_4 NP Fibers. SEM images of PVP fibers loaded with FM NPs (average diameter of 151 nm) are shown in Figure 3. All of the samples had similar fiber diameters around 2 μm at 5 to 50 wt % NP loading. Knot-like features can be seen to increase due to the aggregation of NPs in the fibers with increasing NP loadings, but despite this unfavorable aggregation, continuous fibers up to 50 wt % NP loading were obtained. It is possible that a magnetic interaction played a role in this agglomeration during the electrospinning process, which subjects the solution to very high electrical potentials (above 10 kV). The FM NPs did not have any surfactant coating on their surfaces and this also played a significant role in the agglomerations observed at high loadings.

The SEM images of the electrospun PVP fibers containing mixtures of FM and SPM NPs are shown in Figure 4. The fiber diameters became slightly thinner with increased SPM NP loadings in the fibers, and the fibers showed increased roughness due to the addition of the SPM NPs. However, the TEM images shown in Figure 5 indicate that no obvious aggregation occurred in any of the mixed NP fibers. These favorable fiber characteristics may be due in part to the oleic acid present on the surface of the SPM NPs, which may be removed during the sonication in propanol, and then stabilize the FM NPs in the solution. Another possible mechanism that would result in the thinner more uniform fibers is that the well-dispersed SPM NPs may help stabilize the large FM NPs by physically preventing agglomeration, and creating an improved solution rheology as a result. As compared with 50 wt % FM NP fiber shown in Figure 3e and 50 wt % SPM NP fiber shown in Figure 4a, the aggregation of NPs in the FM fiber was more pronounced.

Figure 5 shows TEM images of various fibers, and also examines both thin and thick fibers to determine the arrangement of the NPs in the fibers. Smaller SPM NPs arrange themselves into clusters in the thinner fiber (Figure 5e), and the thicker fiber has the larger FM NPs surrounded by the much smaller SPM NPs (Figure 5f). The very thin fibers are too small to accommodate the FM NPs that are typically 100 nm in diameter or larger. These very thin fibers account for only a fraction of the observed fibers (as can be seen in the SEM images), and it is desirable to avoid these very thin fibers by optimizing the electrospinning conditions.

The X-ray diffraction (XRD) patterns of a PVP fiber containing mixtures of magnetic NPs are shown in Figure 6. The 50 wt % FM NP-containing fiber exhibited a similar diffraction pattern to those in literature.[36] The Miller index of crystalline diffraction peaks (220), (311), (400), (422), (511), and (440) were found at 2-theta of 30.07, 35.41, 43.09, 53.60, 57.10, and 62.64, respectively. The intensity of these peaks gradually decreased as the concentration of FM NPs was reduced even though the total concentration of NPs were maintained constant at 50 wt %. The pure 50 wt % SPM NP-containing fiber had much lower intensity, broad peaks from crystallite Fe_3O_4 than did the pure 50 wt % FM NP-containing fiber, even though the peak positions remained at the same values of 2θ. On the basis of XRD, the average grain size of

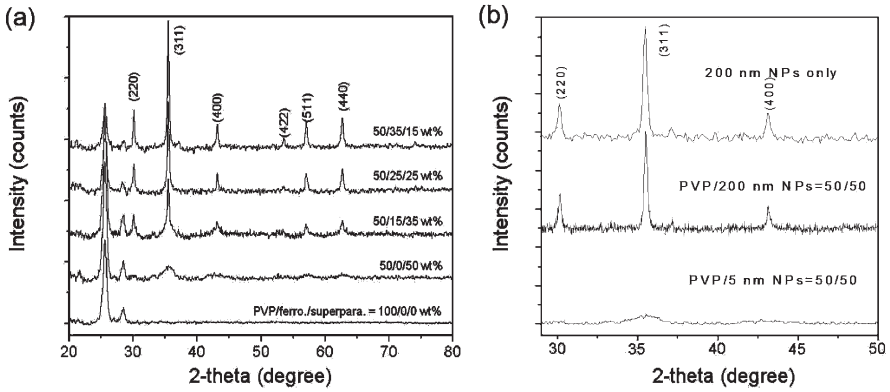

Figure 6. The XRD patterns of (a) PVP fibers containing a mixture of FM NPs and SPM NPs. The XRD pattern of (b) FM NPs before being incorporated into electrospun fibers and the XRD of a fiber containing 50 wt % FM NPs confirms that these large NPs are indeed incorporated into the electrospun fibers. The XRD pattern for a fiber containing 50 wt % SPM NPs is shown (b) for comparison.

Table 1. Diameters of Fe_3O_4 NPs Determined by Both X-ray Diffraction and TEM

sample	D_{XRD} (nm)	D_{TEM} (nm)
FM Fe_3O_4 NPs	41	150.8 ± 59.4
SPM Fe_3O_4 NPs	5.1	5.6 ± 0.6

magnetic NPs could be estimated from the full width at half-maximum (fwhm) of the peaks corresponding to the {311} crystal crystallographic planes using Scherrer's equation (eq 1).[37]

$$D_{hkl} = \frac{k\lambda}{\Omega \cos(\Theta_{hkl})} \quad (1)$$

where D_{hkl} is the average grain size of NPs, k is the form factor ($k = 1$), λ is the X-ray wavelength (0.1542 nm), Ω is the FWHM, and Θ is half of the scattering angle from the {311} plane.

The average grain size from FM and SPM Fe_3O_4 NPs based on the XRD and TEM data suggests that a FM NP consists of multimagnetic domains. The size of each domain in an FM NP as measured by the XRD is well above the critical diameter for Fe_3O_4. As illustrated in the TEM images (Figure 2), FM Fe_3O_4 NPs have a very broad distribution with pronounced aggregation, while the SPM Fe_3O_4 NPs showed much uniform distribution with very little aggregation, because of their oleic acid surface coating. The larger grain size of FM NPs measured by TEM suggests that a FM NP consists of multimagnetic domains. (Table 1).

Magnetic Properties of Electrospun PVP-Fe_3O_4 fibers. The magnetic properties of the electrospun PVP fibers loaded with magnetic NPs were examined at 300 K using a SQUID magnetometer. When the applied magnetic field was low, the formation of a hysteresis loop was clearly observed for all samples, except for the sample loaded with only SPM NPs, as shown in the enhanced view in the upper left inset of Figure 7. These correspond to commonly observed phenomena for FM and SPM materials.

The asymptotes seen at the extremes of the plots are used to determine the saturation magnetization, and it can be seen from the plots that increasing the loading of the FM NPs allows for a larger magnetization of the fibers, although anomalous behavior was noted for the FM/SPM = 70/30 sample. This curve was expected to reach a higher saturation magnetization, a trend that

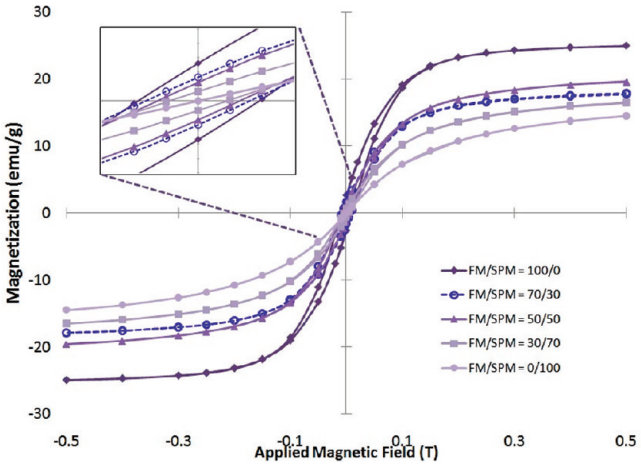

Figure 7. SQUID analysis of electrospun PVP fibers containing 50 wt % magnetic Fe_3O_4 NPs, showing magnetization in electromagnetic units per gram of fiber (emu/g) against the strength of the applied magnetic field in Tesla (T). The NPs loaded into the fibers were FM, SPM, or a mixture of both. The legend shows the percentages of the two NPs relative to the total mass of NPs in the fibers. The data for FM/SPM 70/30 (labeled blue dash with open circle) was anomalous despite repeated experiments, suggesting a possible magnetic interaction at this loading ratio.

was observed for all other samples. The remnant magnetization values did fit the overall trend for this sample, and so the reason for the anomalous behavior in the plot for FM/SPM = 70/30 is not entirely clear. It seems that something unique is occurring in the fibers with this ratio of FM to SPM NPs, but this phenomenon is not understood at this time. The position where the hysteresis loop crosses the y-axis is known as the remnant magnetization, the magnetization remaining after the applied external magnetic field has been completely removed. The remnant magnetization values were compared among the various fibers to determine if there was a mesoscale magnetic exchange coupling interaction between the larger diameter FM NPs and the smaller SPM NPs. It was evident that a significant magnetic interaction resulting in increased remnant magnetization does not occur between these different types of NPs in the electrospun PVP fiber matrix. Although it is possible for SPM NPs to interact with a ferromagnetic matrix, it is possible that the surface coatings

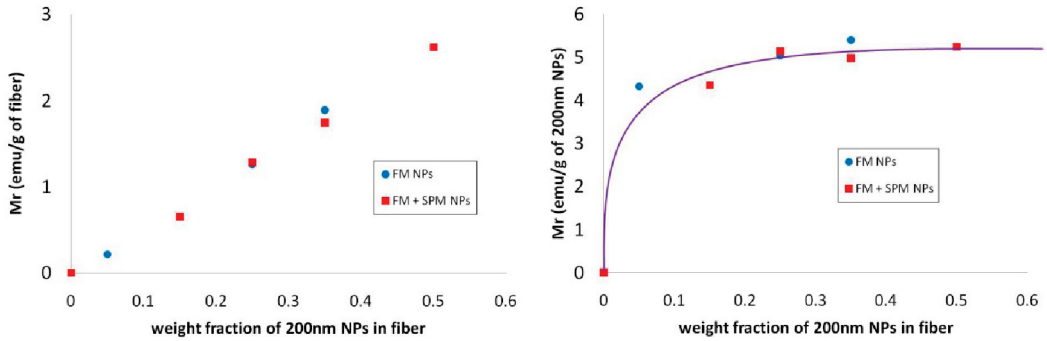

Figure 8. Comparison of the remnant magnetization values relative to fiber weight (left) and FM NP weight (right), for electrospun fibers containing FM NPs and mixtures of FM and SPM NPs. The addition of SPM NPs mixed with FM NPs causes no change in the magnitude or shape of the remnant magnetization relative to the FM NP fibers, despite the presence of significant amounts of SPM NPs (total weight fraction of NPs in mixed fiber was equal to 0.5 in all samples). This suggests that no significant magnetic exchange coupling occurs in the fibers.

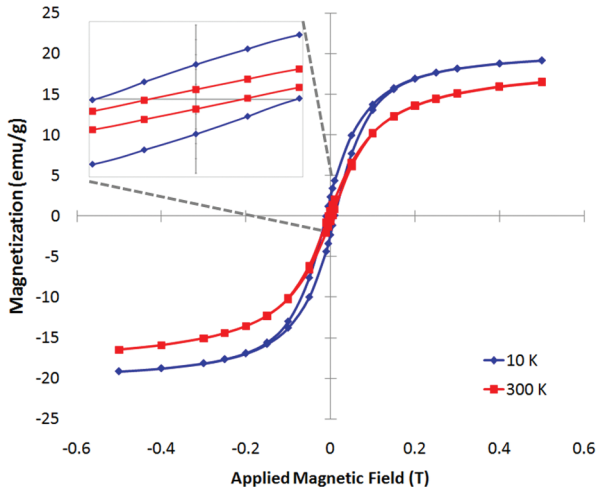

Figure 9. SQUID measurements for an electrospun PVP fiber sample loaded with 50% wt. NPs, and the ratio of these NPs was 30/70 wt % FM/SPM NPs. The low temperature measurement (10 K) shows increases in saturation magnetization, remnant magnetization, and coercivity. This is expected as SPM NPs behave more like FM materials at very low temperatures, which are close to their blocking temperature.

of the nanoparticles or their uniform dispersion in the PVP fibers did not allow them to get sufficiently close to one another to allow for the theoretically predicted magnetic exchange coupling to occur. The fibers loaded with both SPM and FM NPs had properties, which closely matched the FM NP fibers, as illustrated in Figure 8.

FM NPs normally exhibit a linear relation between NPs loading and remnant magnetization. The addition of SPM NPs causes no significant deviation from this behavior due to a lack of a mesoscale magnetic interaction between the FM and SPM NPs. With such high NP loadings, the magnetic properties observed in these fibers suggest that a magnetic coupling of SPM and FM NPs in a polymer matrix may not be possible, despite the fact that previous researchers have shown that enhanced magnetization stability is possible when SPM materials are embedded in a FM matrix.[38] Although it was hypothesized that SPM NPs would magnetically interact on the mesoscale with FM micro and NPs,[39] the present work represents the first experimental examination of whether such interactions take place in a polymer fiber. It is possible, however, that with a proper tuning of the surface stabilizing agents (e.g., oleic acid) and the polymer matrix (e.g., PVP), it might still be possible to achieve a magnetic coupling of SPM NPs with FM NPs. It may be necessary to force the controlled aggregation of the SPM and FM NPs, bringing them sufficiently close to permit for magnetic coupling.

The sample of 30/70 FM/SPM NPs in electrospun PVP fibers was loaded into the SQUID and evaluated at 300 K, and then the temperature was lowered to 10 K, which improved the magnetic properties of the sample and this is shown as Figure 9.

CONCLUSIONS

In summary, electrospinning of mixed magnetic composites may offer an important platform for better understanding the magnetic properties of materials and provide a scalable process for the fabrication of nanocomposites having novel magnetic properties. Future studies will focus on the fabrication and study of single fibers or oriented fiber devices, and the magnetic coupling of SPM NPs with FM NPs in a polymeric matrix may be possible under appropriate controlled aggregation. Further studies of the interaction resulting in the anomalous behavior at a loading ratio of 70/30 FM/SPM may be warranted to elucidate the mechanism and possible applications.

AUTHOR INFORMATION

Corresponding Author

*Phone: 518-276-3404; Fax: 518-276-3405; Email: linhar@rpi.edu.

Author Contributions

†These authors contributed equally to this work.

ACKNOWLEDGMENT

This work was supported by the U.S. National Science Foundation funded Rensselaer Nanotechnology Center as well as Chisso Corporation. The authors are grateful to the Massachusetts Institute of Technology for access to its SQUID facility.

REFERENCES

(1) Terris, B. D.; Thomson, T. *J. Phys. D: Appl. Phys.* **2005**, *38*, R199–R222.

(2) Li, G.; Sun, S.; Wilson, R. J.; White, R. L.; Pourmand, N.; Wang, S. X. *Sensors and Actuators A* **2006**, *126*, 98–106.

(3) Gupta, A. K.; Gupta, M. *Biomaterials* **2005**, *26*, 3995–4021.
(4) Huang, Z. M.; Zhang, Y. Z.; Kotaki, M.; Ramakrishna, S. *Compos. Sci. Technol.* **2003**, *63*, 2223–2253.
(5) Jin, H.; Chen, J.; Karageorgiou, V.; Altman, G. H.; Kaplan, D. L. *Biomaterials* **2004**, *6*, 1039–1047.
(6) Macdiarmid, A. G.; Jones, W. E.; Norris, I. D.; Gao, J.; Johmson, A. T.; Pinto, N. J.; Hone, J.; Han, B.; Ko, F. K.; Okuzaki, H.; Llaguno, M. *Synth. Met.* **2001**, *1*, 27–30(4). Kim, C.; Yang, K. S. *Appl. Phys. Lett.* **2003**, *6*, 1216–1218.
(7) Kim, C.; Yang, K. S. *Appl. Phys. Lett.* **2003**, *6*, 1216–1218.
(8) Drew, C.; Liu, X.; Ziegler, D.; Wang, X.; Bruno, F. F.; Whitten, J.; Samuelson, L. A.; Kumar, J. *Nano Lett.* **2003**, *2*, 143–147.
(9) Tsai, P.; Schreuder-Gibson, H.; Gibson, P. *J. Electrost.* **2002**, *3*, 333–341.
(10) Shao, C.; Kim, H.; Gong, J.; Ding, B.; Lee, D.; Park, S. *Mater. Lett.* **2003**, *9*, 1579–1584.
(11) Li, D.; Xia, Y. N. *Adv. Mater.* **2004**, *16*, 1151–1170.
(12) Ko, F.; Gogotsi, Y.; Ali, A.; Naguib, N.; Ye, H.; Yang, G.; Li, C.; Willis, P. *Adv. Mater.* **2003**, *15*, 1161–1165.
(13) Miyauchi, M.; Miao, J. J.; Simmons, T. J.; Lee, J. W.; Doherty, T. V.; Dordick, J. S.; Linhardt, R. J. *Biomacromolecules* **2010**, *11*, 2440–2445.
(14) Formo, E.; Lee, E.; Campbell, D.; Xia, Y. N. *Nano Lett.* **2008**, *8* (2), 668–672.
(15) Son, W. K.; Youk, J. H.; Park, W. H. *Carbohydr. Polym.* **2006**, *65* (4), 430–434.
(16) Wang, M.; Singh, H.; Hatton, T. A.; Rutledge, G. C. *Polymer* **2004**, *45*, 5505–5514.
(17) Pinchuk, L. S.; Markova, L. V.; Gromyko, Y. V.; Markov, E. M.; Choi, J. *Mater. Process technol.* **1995**, *55*, 345–350.
(18) Epstein, A. J.; Miller, J. S. *Synth. Met.* **1996**, *80*, 231–237.
(19) Dikeakos, M.; Tung, L. D.; Veres, T.; Stancu, A.; Spinu, L.; Normandin, F. *Proc. Mater. Res. Soc.* **2003**, *734*, 315–320.
(20) Chatterjee, J; Haik, Y; Chen, C.-J. *J. Magn. Magn. Mater.* **2003**, *257* (1), 113–8.
(21) Sato, T; Iijima, T; Sekin, M; Inagaki, N. *J. Magn. Magn. Mater.* **1987**, *65*, 252–256.
(22) Atsumi, T.; Jeyadevan, B.; Sato, Y.; Tohji, K. *J. Magn. Magn. Mater.* **2007**, *310*, 2841–2843.
(23) Wang, M.; Singh, H.; Hatton, T. A.; Rutledge, G. C. *Polymer* **2004**, *45*, 5505–5514.
(24) Tan, S. T.; Wendorff, J. H.; Pietzonka, C.; Jia, Z. H.; Wang, G. Q. *Chem. Phys. Chem.* **2005**, *6*, 1461–1465.
(25) Kalra, V.; Lee, J.; Lee, J. H.; Lee, G.; Marquez, M.; Wiesner, U.; Joo, Y. L. *Small* **2008**, *11*, 2067–2073.
(26) Mincheva, R.; Stoilova, O.; Penchev, H.; Ruskov, T.; Spirov, I.; Manolova, N.; Rashkov, I. *Eur. Polym. J.* **2008**, *44*, 615–627.
(27) Zhang, D.; Karki, A. B.; Rutman, D.; Young, D. P.; Wang, A.; Cocke, D.; Ho, T. H.; Guo, Z. *Polymer* **2009**, *50*, 4189–4198.
(28) Lin, C. R.; Tsai, T. C.; Chung, M.; Lu, S. Z. *J. Appl. Phys.* **2009**, *105*, 07B509.
(29) Gupta, P.; Ramazan, A.; Claus, R.; Wilkes, G. *J. Appl. Polym. Sci.* **2006**, *100*, 4935–4942.
(30) Wang, H.; Tang, H; He, J.; Wang, Q. *Mater. Res. Bull.* **2009**, *44*, 1676–1680.
(31) Jin, Y.; Lu, X.; Wang, C. *J. Appl. Polym. Sci.* **2006**, *102*, 6017.
(32) Kessick, R.; Tepper, G. *Sens. Actuators, B* **2006**, *117*, 205–210.
(33) Lu, X.; Zhang, W.; Zhao, Q.; Wang, L.; Wang, C. *e-Polym.* **2006**, No. 033
(34) Li, X.; Wang, C.; Li, Y.; Chu, H. B.; Li, L. *J. Solid State Phenom.* **2007**, *121*, 109–112.
(35) Chuangchote, S.; Sagawa, T.; Yoshik, S. *J. Appl. Polym. Sci.* **2009**, *114*, 2777–2791.
(36) Sharma, N.; Jaffari, G. H.; Shah, S. I.; Pochan, D. J. *Nanotechnology* **2010**, *21*, No. 085707.
(37) Scherrer, P. *Nachr. Ges. Wiss. Göttingen, Math.-Phys. Kl.* **1918**, *2*, 98–100.
(38) Vargas, J. M.; Gómez, J.; Zysler, R. D.; Butera, A. *Nanotechnology* **2007**, *18*, No. 115714.
(39) Safonov, V. L.; Bertram, H. N. *J. Appl. Phys.* **2003**, *93* (10), 8474–8476.